Cell Reports Medicine, Volume *2*

Supplemental information

A GPC2 antibody-drug conjugate is efficacious against neuroblastoma and small-cell lung cancer via binding a conformational epitope

Swetha Raman, Samantha N. Buongervino, Maria V. Lane, Doncho V. Zhelev, Zhongyu Zhu, Hong Cui, Benjamin Martinez, Daniel Martinez, Yanping Wang, Kristen Upton, Khushbu Patel, Komal S. Rathi, Carmen T. Navia, Daniel B. Harmon, Yimei Li, Bruce Pawel, Dimiter S. Dimitrov, John M. Maris, Jean-Philippe Julien, and Kristopher R. Bosse

Figure S1

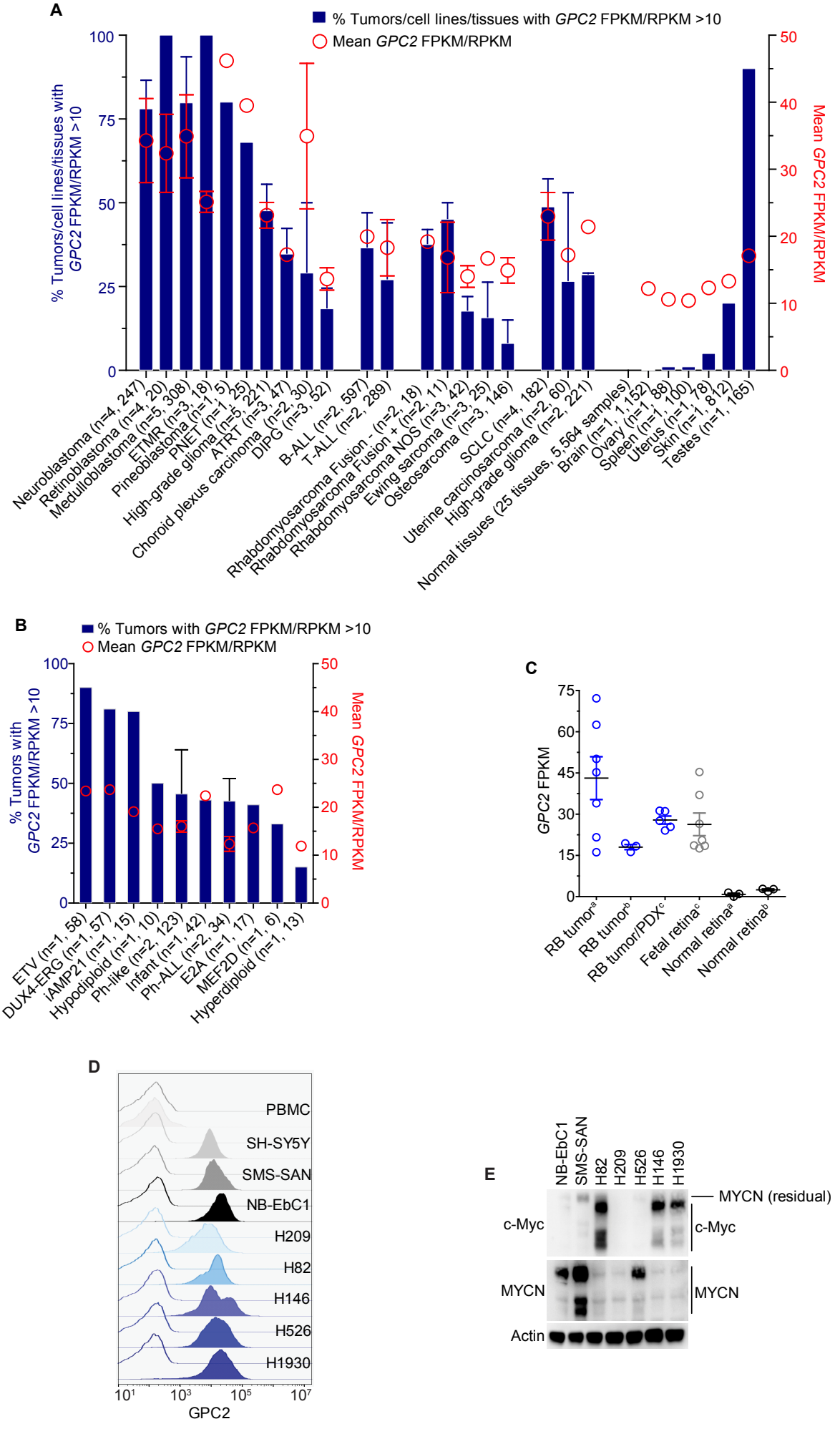
A
% Tumors/cell lines/tissues with GPC2 FPKM/RPKM >10
Mean GPC2 FPKM/RPKM
% Tumors/cell lines/tissues with GPC2 FPKM/RPKM >10
Mean GPC2 FPKM/RPKM
Neuroblastoma (n=4, 247)
Retinoblastoma (n=4, 20)
Medulloblastoma (n=5, 308)
ETMR (n=3, 18)
Pineoblastoma (n=1, 5)
PNET (n=1, 25)
High-grade glioma (n=5, 221)
ATRT (n=3, 47)
Choroid plexus carcinoma (n=2, 30)
DIPG (n=3, 52)
B-ALL (n=2, 597)
T-ALL (n=2, 289)
Rhabdomyosarcoma Fusion - (n=2, 18)
Rhabdomyosarcoma Fusion + (n=2, 11)
Rhabdomyosarcoma NOS (n=3, 42)
Ewing sarcoma (n=3, 25)
Osteosarcoma (n=3, 146)
SCLC (n=4, 182)
Uterine carcinosarcoma (n=2, 60)
High-grade glioma (n=2, 221)
Normal tissues (25 tissues, 5,564 samples)
Brain (n=1, 1,152)
Ovary (n=1, 88)
Spleen (n=1, 100)
Uterus (n=1, 78)
Skin (n=1, 812)
Testes (n=1, 165)
B
% Tumors with GPC2 FPKM/RPKM >10
Mean GPC2 FPKM/RPKM
% Tumors with GPC2 FPKM/RPKM >10
Mean GPC2 FPKM/RPKM
ETV (n=1, 58)
DUX4-ERG (n=1, 57)
iAMP21 (n=1, 15)
Hypodiploid (n=1, 10)
Ph-like (n=2, 123)
Infant (n=1, 42)
Ph-ALL (n=2, 34)
E2A (n=1, 17)
MEF2D (n=1, 6)
Hyperdiploid (n=1, 13)
C
GPC2 FPKM
RB tumor[a]
RB tumor[b]
RB tumor/PDX[c]
Fetal retina[c]
Normal retina[a]
Normal retina[b]
D
PBMC
SH-SY5Y
SMS-SAN
NB-EbC1
H209
H82
H146
H526
H1930
GPC2
E
NB-EbC1
SMS-SAN
H82
H209
H526
H146
H1930
MYCN (residual)
c-Myc
c-Myc
MYCN
MYCN
Actin

Figure S1. *GPC2* is developmentally regulated and highly expressed in other pediatric and adult cancers. Related to Figure 1.

(**A**) Summary plot of *GPC2* RNA sequencing data across pediatric and adult tumor datasets. The blue bars graphed on the left y-axis represent the % of tumors/cell lines/normal tissues with *GPC2* FPKM/RPKM >10 represented as mean ± SEM of multiple data sets per tumor histotype or normal tissue as indicated (n=1-5 datasets per tumor/cell line/tissue). The red circles graphed on the right y-axis represent the mean *GPC2* FPKM/RPKM ± SEM of the >10 FPKM/RPKM cohort of tumors/cell lines/normal tissues in each data set. The number of data sets and total samples for each tumor histotype/normal tissue is indicated on the x-axis (n=total data sets, total tumors/cell lines/tissues).

(**B**) Summary plot of *GPC2* RNA sequencing data across pediatric ALL subtypes. The blue bars graphed on the left y-axis represent the % of ALLs with *GPC2* FPKM/RPKM >10 represented as mean ± SEM of multiple data sets per ALL subtype as indicated. The red circles graphed on the right y-axis represent the mean *GPC2* FPKM/RPKM ± SEM of the >10 FPKM/RPKM cohort of ALLs in each data set. The number of data sets and total samples for each ALL subtype is indicated on the x-axis (n=total data sets, total tumors).

(**C**) *GPC2* expression in retinoblastomas, fetal and normal retinas represented as mean ± SEM with each circle representing an individual sample. [a]Normal retina and retinoblastoma data from GSE125903[1]; [b]Normal retina and retinoblastoma data from GSE111168[2]; [c]Normal fetal retina and retinoblastoma tumor and PDX data from GSE87042.[3]

(**D**) Representative GPC2 flow cytometry histograms of neuroblastoma and SCLC cell lines. SH-SY5Y, SMS-SAN and NB-EbC1 are representative neuroblastoma cell lines.

(**E**) c-Myc and MYCN Western blot of SCLC and neuroblastoma cell lines. SMS-SAN and NB-EbC1 are representative neuroblastoma cell lines.

ETMR, embryonal tumor with multilayered rosettes; PNET, primitive neuroectodermal tumor; ATRT, atypical teratoid rhabdoid tumor; DIPG, diffuse intrinsic pontine glioma; NOS, not-otherwise specified; SCLC, small cell lung cancer; RB, retinoblastoma; PBMC, peripheral blood mononuclear cell.

Figure S2

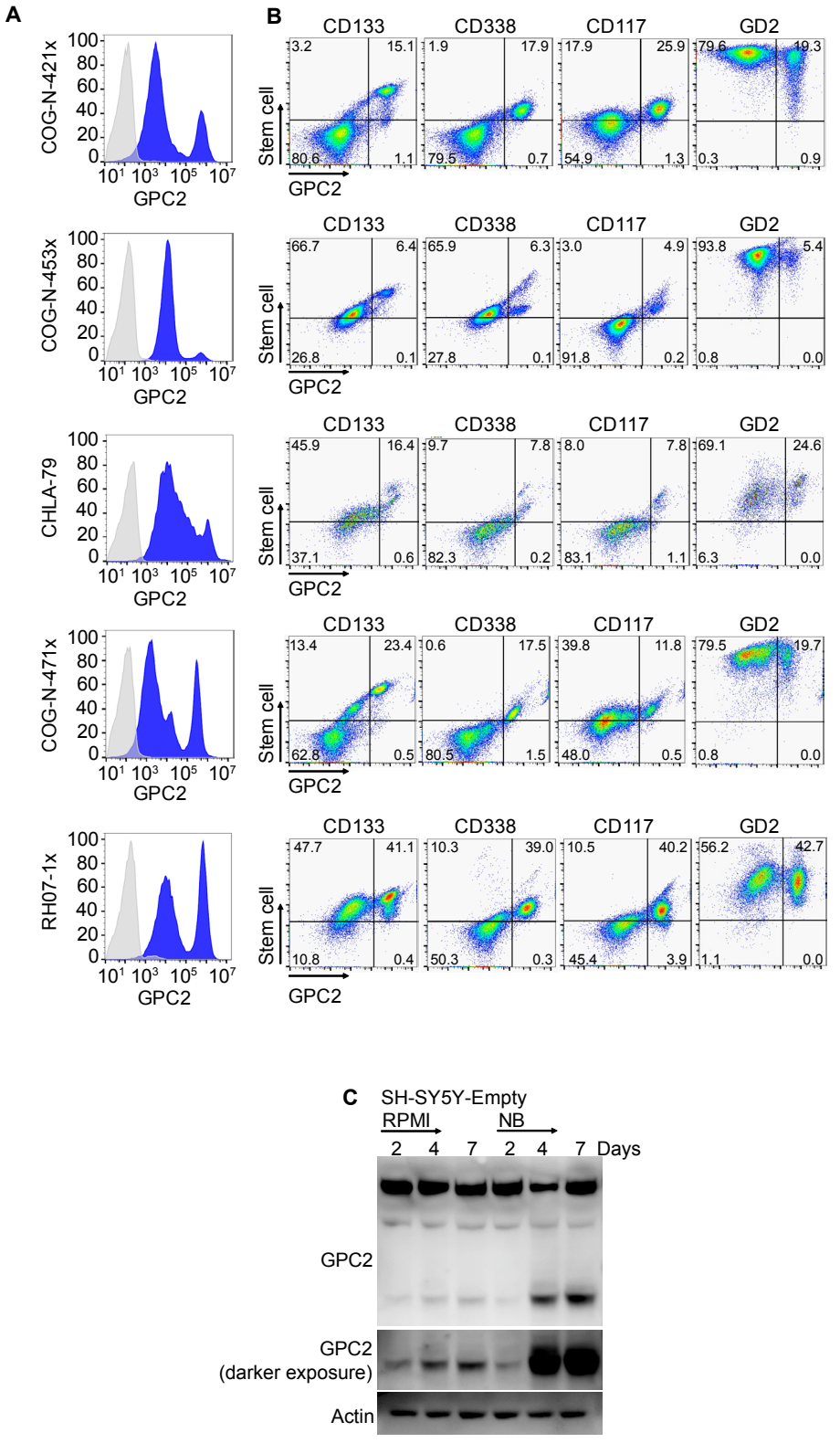
A
B
COG-N-421x
COG-N-453x
CHLA-79
COG-N-471x
RH07-1x
GPC2
Stem cell
CD133
CD338
CD117
GD2
3.2
15.1
80.6
1.1
1.9
17.9
79.5
0.7
17.9
25.9
54.9
1.3
79.6
19.3
0.3
0.9
66.7
6.4
26.8
0.1
65.9
6.3
27.8
0.1
3.0
4.9
91.8
0.2
93.8
5.4
0.8
0.0
45.9
16.4
37.1
0.6
9.7
7.8
82.3
0.2
8.0
7.8
83.1
1.1
69.1
24.6
6.3
0.0
13.4
23.4
62.8
0.5
0.6
17.5
80.5
1.5
39.8
11.8
48.0
0.5
79.5
19.7
0.8
0.0
47.7
41.1
10.8
0.4
10.3
39.0
50.3
0.3
10.5
40.2
45.4
3.9
56.2
42.7
1.1
0.0
C
SH-SY5Y-Empty
RPMI
NB
2 4 7 2 4 7 Days
GPC2
GPC2
(darker exposure)
Actin

Figure S2. GPC2 is a putative neuroblastoma stem cell marker. Related to Figure 2.

(**A**, **B**) GPC2 flow cytometry histograms (**A**) and GPC2 vs. CD133, CD338, CD117 and GD2 plots (**B**) of neuroblastoma PDXs (COG-N-421x, COG-N-453x, COG-N-471x and RH07-1x) and cell line xenograft (CHLA-79).

(**C**) GPC2 Western blot of SH-SY5Y-Empty^{RPMI} vs. SH-SY5Y-Empty^{NB} cells.

Figure S3

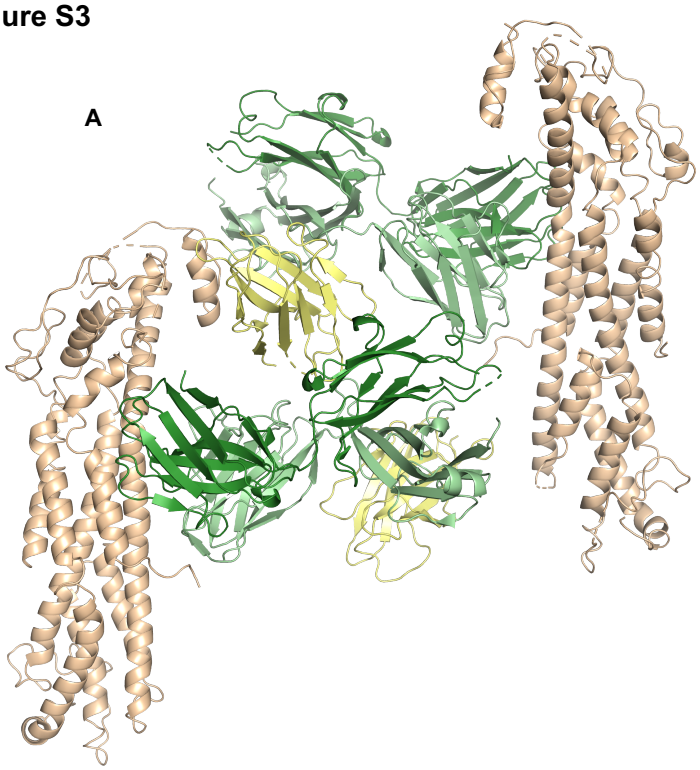
A


B

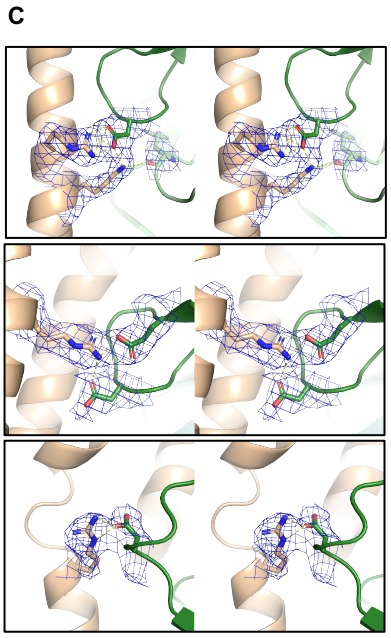
C

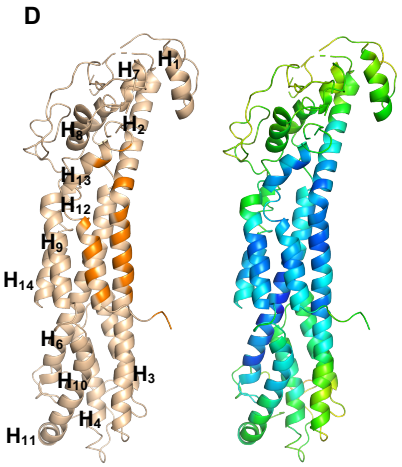
D
H7
H1
H8
H2
H13
H12
H9
H14
H6
H10
H3
H4
H11

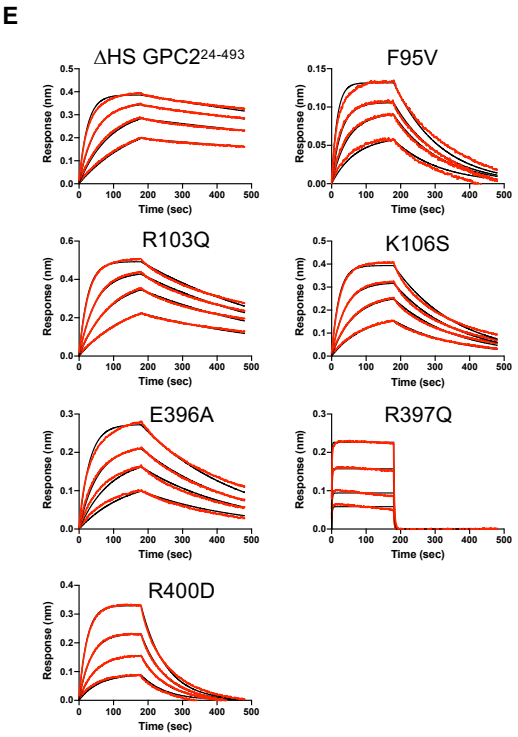
E
ΔHS GPC2 24-493
F95V
R103Q
K106S
E396A
R397Q
R400D
Response (nm)
Time (sec)

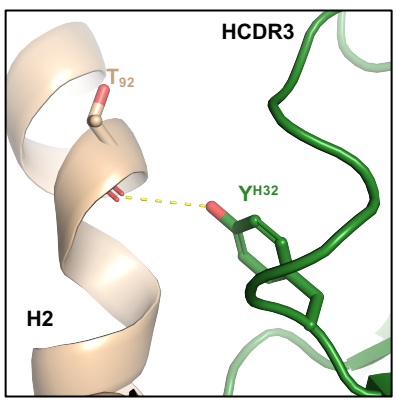
F
HCDR3
T92
YH32
H2

Figure S3. The D3-GPC2-Fab binds a conformational GPC2 protein epitope. Related to Figure 3.

(**A**) Overview of the co-crystal structure that shows two NCS-related copies of the D3-GPC2-Fab/ΔHS GPC2$^{24-493}$ complex in the asymmetric unit. GPC2 is shown in wheat, the D3-GPC2-Fab in green and the V_HH domain utilized to aid in crystallization in yellow.

(**B**) Superposition of the GPC1 crystal structure (PDB ID: 4ACR, pink) on the GPC2 structure (orange), shown as Cα trace.

(**C**) Stereo images of D3-GPC2-Fab residues (green) interacting with GPC2 residues (wheat). The $2F_o$- F_c map (blue mesh) is rendered at a 1.0 σ contour level. Interactions: GPC2-R103 and -K106 with Fab_{HC}-D99 and Fab_{LC}-L91 (top); GPC2-R397 with Fab_{HC}-E95 and -D99 (middle); GPC2-R400 with Fab_{HC}-D31 (bottom).

(**D**) GPC2 with helices numbered and D3-GPC2-Fab epitope traced in orange (left) and GPC2 colored based on B-factors (right). The color spectrum ranges from B-factors of 30 Å^2 (blue) to 150 Å^2 (orange), with colder colors indicative of regions of overall lower flexibility, such as the D3-GPC2-Fab epitope.

(**E**) Representative kinetics plots showing the binding of D3-GPC2-Fab to the ΔHS GPC2$^{24-493}$ protein and its respective point mutants. The data (red) is fitted with a 1:1 model (black).

(**F**) The Ser/Thr92 interaction (wheat) with heavy chain residues of D3-GPC2-Fab (green).

Figure S4

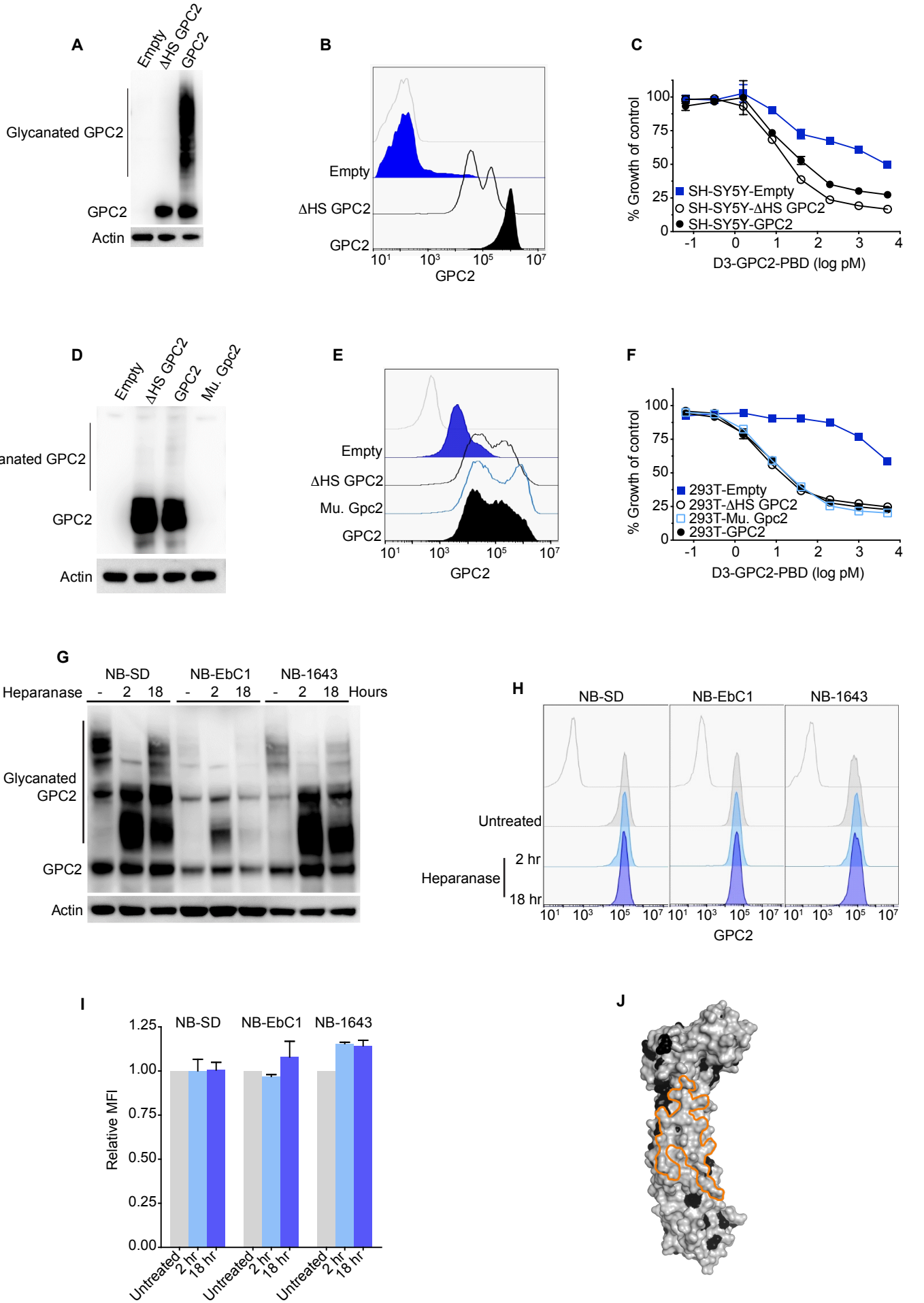
A
Empty
ΔHS GPC2
GPC2
Glycanated GPC2
GPC2
Actin
B
Empty
ΔHS GPC2
GPC2
GPC2
C
% Growth of control
SH-SY5Y-Empty
SH-SY5Y-ΔHS GPC2
SH-SY5Y-GPC2
D3-GPC2-PBD (log pM)
D
Empty
ΔHS GPC2
GPC2
Mu. Gpc2
Glycanated GPC2
GPC2
Actin
E
Empty
ΔHS GPC2
Mu. Gpc2
GPC2
GPC2
F
% Growth of control
293T-Empty
293T-ΔHS GPC2
293T-Mu. Gpc2
293T-GPC2
D3-GPC2-PBD (log pM)
G
NB-SD
NB-EbC1
NB-1643
Heparanase
Hours
Glycanated GPC2
GPC2
Actin
H
NB-SD
NB-EbC1
NB-1643
Untreated
Heparanase
2 hr
18 hr
GPC2
I
NB-SD
NB-EbC1
NB-1643
Relative MFI
Untreated
2 hr
18 hr
J

Figure S4. GPC2-associated heparan sulfate chains do not significantly alter D3-GPC2 antibody binding. Related to Figure 3.

(**A**-**C**) GPC2 Western blot (**A**), D3-GPC2-IgG1 flow cytometry histograms (**B**) and relative growth plots 4 days after treatment with D3-GPC2-PBD (**C**) of SH-SY5Y-Empty, -GPC2 and -ΔHS GPC2 isogenic cells.

(**D**-**F**) GPC2 Western blot (**D**), D3-GPC2-IgG1 flow cytometry histograms (**E**) and relative growth plots 4 days after treatment with D3-GPC2-PBD (**F**) of HEK293T-Empty, -murine Gpc2, -human GPC2 and -ΔHS GPC2 transfected cells. GPC2 antibody used in Western blot in **D** does not recognize murine Gpc2.

(**G**) GPC2 Western blot of neuroblastoma cells after treatment with recombinant heparanase.

(**H**) Representative D3-GPC2-IgG1 flow cytometry histograms of heparanase treated neuroblastoma cells.

(**I**) Summary of relative GPC2 MFIs of heparanase treated neuroblastoma cells from **H**.

(**J**) Human and mouse GPC2 sequence conservation mapped on human GPC2 crystal structure, with variable amino acid residues in black and the D3-GPC2-Fab epitope residues outlined in orange.

Data in **I** is represented as mean ± SEM of two independent replicates. Data in **C** and **F** is represented as mean ± SEM from a representative experiment done in technical triplicate with each experiment being done two independent times.

Figure S5

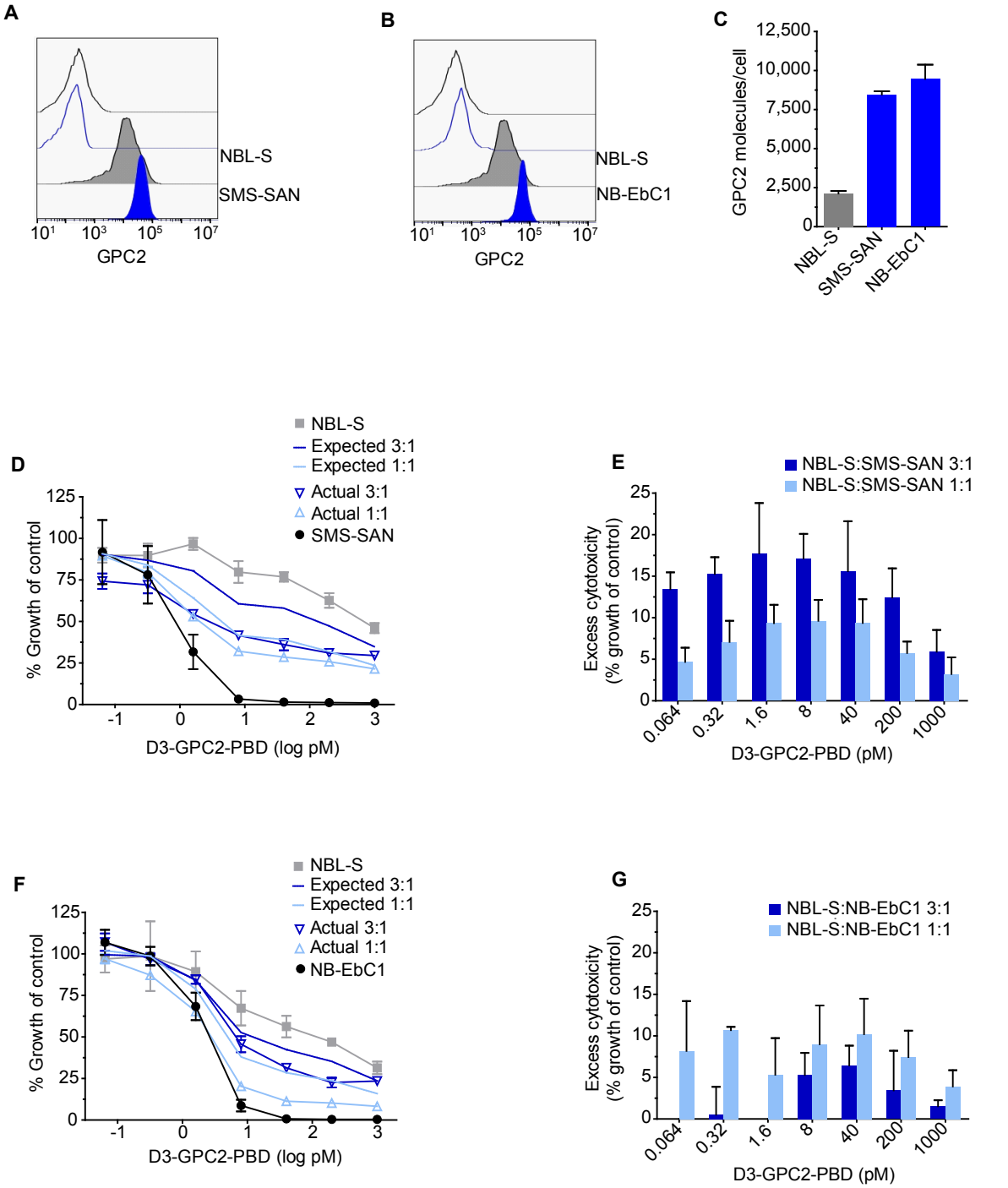
A
NBL-S
SMS-SAN
GPC2
B
NBL-S
NB-EbC1
GPC2
C
GPC2 molecules/cell
12,500
10,000
7,500
5,000
2,500
0
NBL-S
SMS-SAN
NB-EbC1
D
NBL-S
Expected 3:1
Expected 1:1
Actual 3:1
Actual 1:1
SMS-SAN
% Growth of control
D3-GPC2-PBD (log pM)
E
NBL-S:SMS-SAN 3:1
NBL-S:SMS-SAN 1:1
Excess cytotoxicity (% growth of control)
D3-GPC2-PBD (pM)
F
NBL-S
Expected 3:1
Expected 1:1
Actual 3:1
Actual 1:1
NB-EbC1
% Growth of control
D3-GPC2-PBD (log pM)
G
NBL-S:NB-EbC1 3:1
NBL-S:NB-EbC1 1:1
Excess cytotoxicity (% growth of control)
D3-GPC2-PBD (pM)

Figure S5. The D3-GPC2-PBD ADC induces bystander cell killing in paired high/low-GPC2 expressing neuroblastoma cell lines. Related to Figure 4.

(**A**, **B**) Representative GPC2 flow cytometry histograms of NBL-S and SMS-SAN (**A**) and NBL-S and NB-EbC1 (**B**) neuroblastoma cells.

(**C**) GPC2 molecules/cell for NBL-S, NB-EbC1 and SMS-SAN neuroblastoma cells.

(**D**) Representative actual and expected relative growth plots of indicated ratios of NBL-S/SMS-SAN co-incubated cells 6 days after treatment with the D3-GPC2-PBD ADC.

(**E**) Summary plot of excess cytotoxicity observed in co-incubated NBL-S/SMS-SAN cells.

(**F**) Representative actual and expected relative growth plots of indicated ratios of NBL-S/NB-EbC1 co-incubated cells 6 days after treatment with the D3-GPC2-PBD ADC.

(**G**) Summary plot of excess cytotoxicity observed in co-incubated NBL-S/NB-EbC1 cells.

Data in **C**, **E** and **G** is represented as mean ± SEM of 2-3 independent replicates. Data in **D** and **F** is represented as mean ± SEM from a representative experiment done in technical duplicate with each experiment being done at least two independent times.

Figure S6

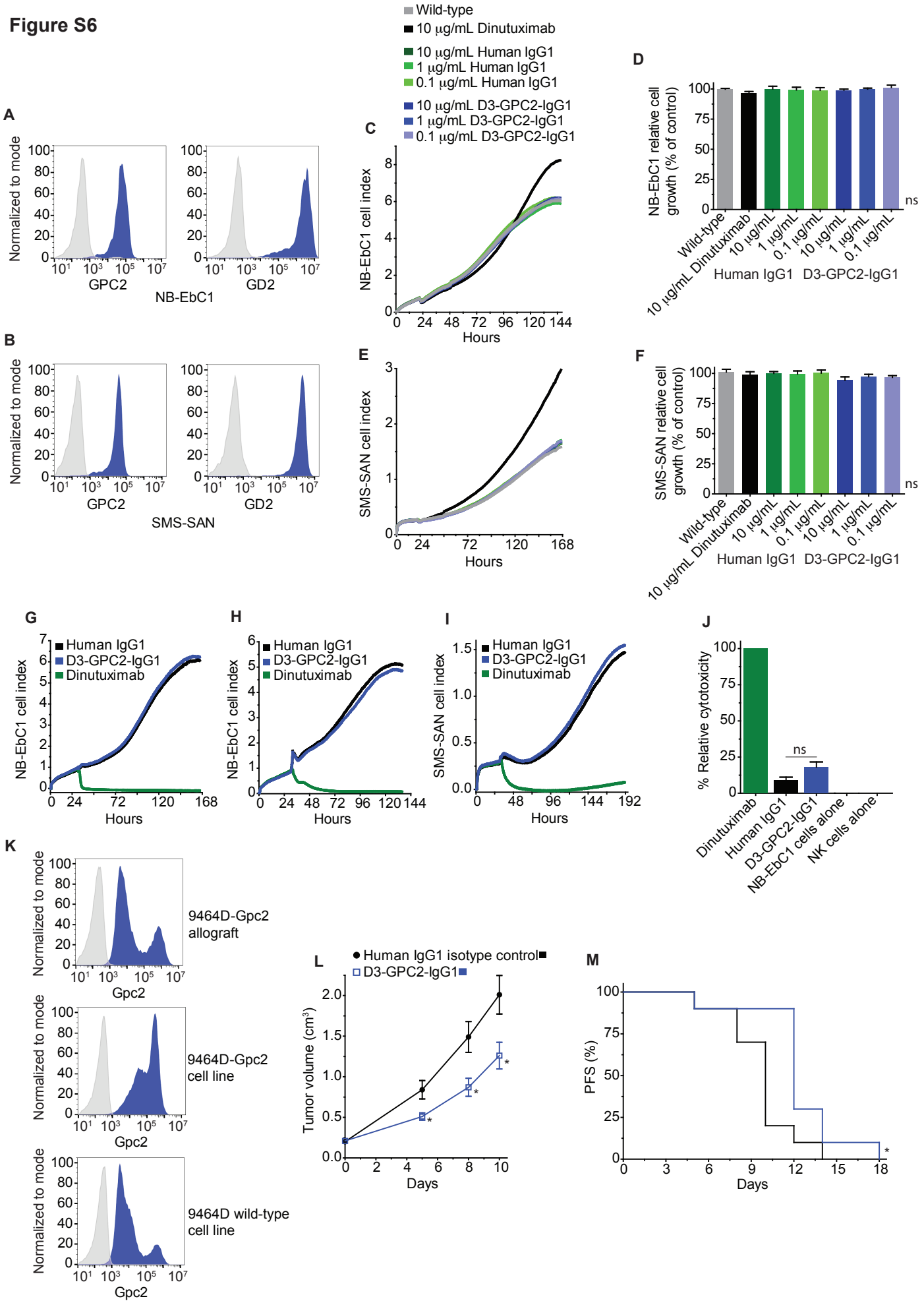
A
Normalized to mode
GPC2
GD2
NB-EbC1
B
SMS-SAN
C
Wild-type
10 μg/mL Dinutuximab
10 μg/mL Human IgG1
1 μg/mL Human IgG1
0.1 μg/mL Human IgG1
10 μg/mL D3-GPC2-IgG1
1 μg/mL D3-GPC2-IgG1
0.1 μg/mL D3-GPC2-IgG1
NB-EbC1 cell index
Hours
D
NB-EbC1 relative cell growth (% of control)
ns
Human IgG1
D3-GPC2-IgG1
E
SMS-SAN cell index
F
SMS-SAN relative cell growth (% of control)
G
Human IgG1
D3-GPC2-IgG1
Dinutuximab
H
I
J
% Relative cytotoxicity
Dinutuximab
Human IgG1
D3-GPC2-IgG1
NB-EbC1 cells alone
NK cells alone
K
9464D-Gpc2 allograft
9464D-Gpc2 cell line
9464D wild-type cell line
Gpc2
L
Human IgG1 isotype control
D3-GPC2-IgG1
Tumor volume (cm3)
Days
M
PFS (%)

Figure S6. The D3-GPC2-IgG1 antibody alone does not significantly inhibit neuroblastoma cell growth or induce ADCC. Related to Figures 3 and 4.

(**A**) NB-EbC1 GPC2 (left) and GD2 (right) flow cytometry histograms.

(**B**) SMS-SAN GPC2 (left) and GD2 (right) flow cytometry histograms.

(**C**, **D**) NB-EbC1 cell growth after treatment with D3-GPC2-IgG1 as measured by RT-CES (**C**) or CellTiter-Glo® assay (**D**).

(**E**, **F**) SMS-SAN cell growth after treatment with D3-GPC2-IgG1 as measured by RT-CES (**E**) or CellTiter-Glo® assay (**F**).

(**G**, **H**) NB-EbC1 cell growth after treatment with D3-GPC2-IgG1 and co-incubation with human NK cells (**G**) or PBMCs (**H**).

(**I**) SMS-SAN cell growth after treatment with D3-GPC2-IgG1 and co-incubation with human NK cells.

(**J**) NB-EbC1 relative cytotoxicity after treatment with D3-GPC2-IgG1 and co-incubation with human NK cells as measured by an LDH-Glo™ cytotoxicity assay.

(**K**) Murine neuroblastoma cell line 9464D, isogenic cell line 9464D-Gpc2 and 9464D-Gpc2 allograft Gpc2 flow cytometry histograms.

(**L**, **M**) Tumor growth of 9464D-Gpc2 allografts treated with D3-GPC2-IgG1 (n=10 mice/cohort; represented as mean ± SEM; **L**) and corresponding progression-free survival (PFS; **M**).

Data in **C**-**J** is represented as either mean or mean ± SEM from representative experiments done in at least technical duplicate at least two independent times. ns, not significant; *, $p < 0.05$.

Figure S7

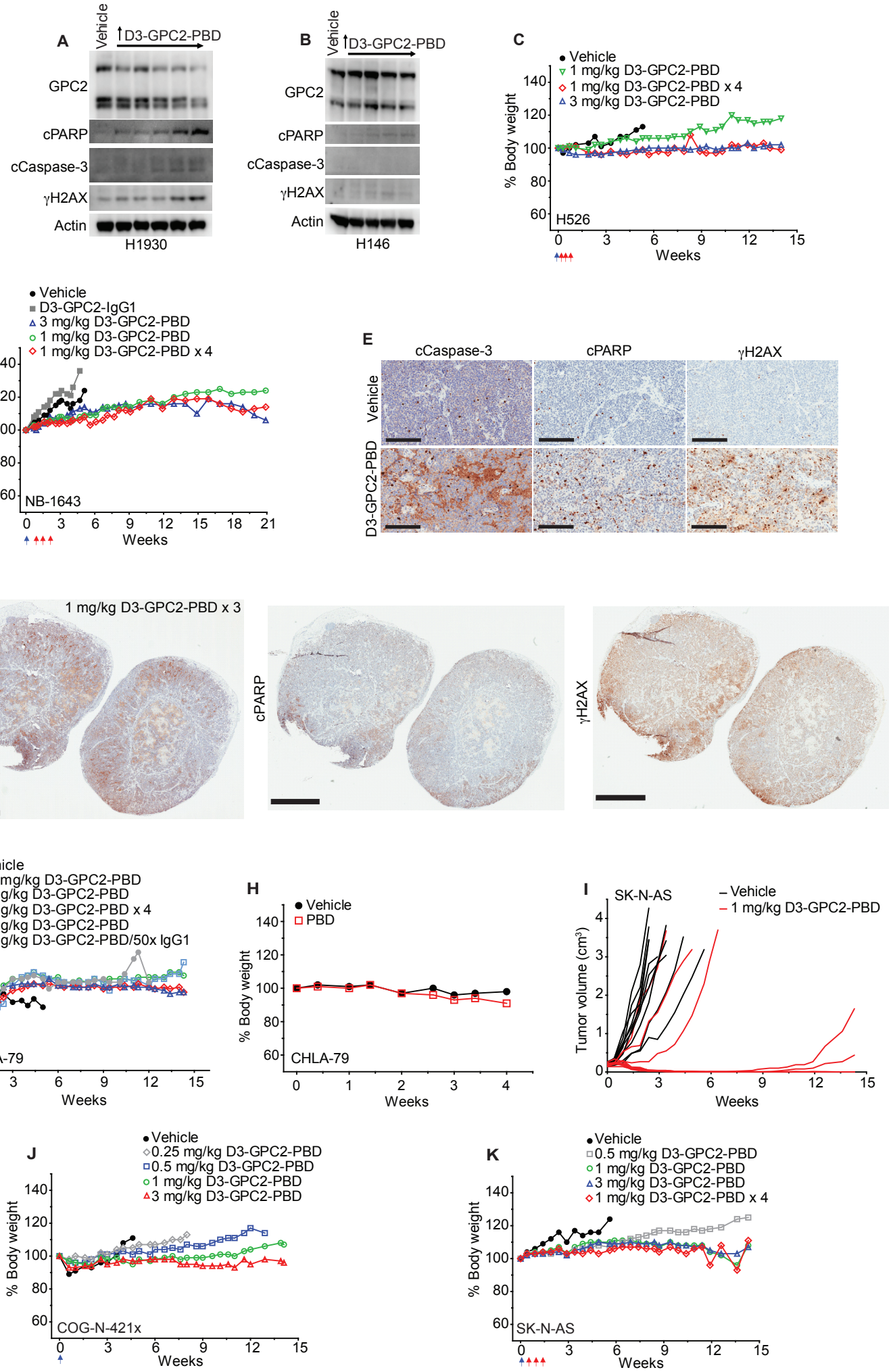
A
Vehicle
D3-GPC2-PBD
GPC2
cPARP
cCaspase-3
γH2AX
Actin
H1930
B
Vehicle
D3-GPC2-PBD
GPC2
cPARP
cCaspase-3
γH2AX
Actin
H146
C
Vehicle
1 mg/kg D3-GPC2-PBD
1 mg/kg D3-GPC2-PBD x 4
3 mg/kg D3-GPC2-PBD
% Body weight
H526
Weeks
D
Vehicle
D3-GPC2-IgG1
3 mg/kg D3-GPC2-PBD
1 mg/kg D3-GPC2-PBD
1 mg/kg D3-GPC2-PBD x 4
% Body weight
NB-1643
Weeks
E
cCaspase-3
cPARP
γH2AX
Vehicle
D3-GPC2-PBD
F
1 mg/kg D3-GPC2-PBD x 3
cCaspase-3
cPARP
γH2AX
G
Vehicle
0.5 mg/kg D3-GPC2-PBD
1 mg/kg D3-GPC2-PBD
1 mg/kg D3-GPC2-PBD x 4
3 mg/kg D3-GPC2-PBD
1 mg/kg D3-GPC2-PBD/50x IgG1
% Body weight
CHLA-79
Weeks
H
Vehicle
PBD
% Body weight
CHLA-79
Weeks
I
SK-N-AS
Vehicle
1 mg/kg D3-GPC2-PBD
Tumor volume (cm³)
Weeks
J
Vehicle
0.25 mg/kg D3-GPC2-PBD
0.5 mg/kg D3-GPC2-PBD
1 mg/kg D3-GPC2-PBD
3 mg/kg D3-GPC2-PBD
% Body weight
COG-N-421x
Weeks
K
Vehicle
0.5 mg/kg D3-GPC2-PBD
1 mg/kg D3-GPC2-PBD
3 mg/kg D3-GPC2-PBD
1 mg/kg D3-GPC2-PBD x 4
% Body weight
SK-N-AS
Weeks

Figure S7. The D3-GPC2-PBD ADC induces diffuse intratumoral DNA damage and apoptosis without any systemic side effects in SCLC and neuroblastoma *in vivo* murine models. Related to Figures 5, 6 and 7.

(**A**) Western blot of H1930 SCLC cells 3 days after treatment with D3-GPC2-PBD (1.6, 8, 40, 200 and 1000 pM).

(**B**) Western blot of H146 SCLC cells 3 days after treatment with D3-GPC2-PBD (1.6, 8, 40 and 200 pM).

(**C**) Mean percent body weights from baseline of mice in the SCLC H526 xenograft treatment arms shown in **Fig. 5E**.

(**D**) Mean percent body weights from baseline of mice in the NB-1643 PDX treatment arms shown in **Fig. 6A**.

(**E**) High-power images of cCaspase-3, cPARP and γH2AX IHC of locally advanced NB-1643 PDX tumors after treatment with 1 mg/kg D3-GPC2-PBD x 3 (ADC dosed on study days 0, 3 and 7 and tumor collected on day 9; also see **Fig. 6C**-**F**).

(**F**) Low-power images of cCaspase-3, cPARP and γH2AX IHC of locally advanced NB-1643 PDX tumors after treatment with 1 mg/kg D3-GPC2-PBD x 3 (ADC dosed on study days 0, 3 and 7 and tumor collected on day 9).

(**G**) Mean percent body weights from baseline of mice of the CHLA-79 xenograft treatment arms shown in **Fig. 6G**.

(**H**) Mean percent body weights from baseline of mice in the CHLA-79 xenograft treatment arms shown in **Fig. 6L.**

(**I**) Individual tumor growth curves for SKNAS xenografts after treatment with vehicle or 1 mg/kg D3-GPC2-PBD ADC. Also shown in summary form in **Fig. 7G.**

(**J**) Mean percent body weights from baseline of mice in the COG-N-421x PDX treatment arms shown in **Fig. 7A**.

(**K**) Mean percent body weights from baseline of mice in the SK-N-AS treatment arms shown in **Fig. 7G**.

Scale bars in **E** represent 200 μM and **F** represent 3 mM. Blue arrows in **C**, **D**, **G, J** and **K** represent initial ADC dose and red arrows in **C**, **D, G** and **K** indicate subsequent 3 ADC doses for the 1 mg/kg ADC x 4 treatment cohort.

Table S1. Summary of SCLC D3-GPC2-PBD/PBD IC_{50} data and *GPC2*/*MYC* family expression. Related to Figures 1 and 5.

Cell line	D3-GPC2-PBD IC_{50} ± SEM (pM)	PBD IC_{50} ± SEM (pM)	TP53 mutation[a]	*GPC2* RPKM[a]	*MYCN* RPKM[a]	*MYC* RPKM[a]	*MYCL* RPKM[a]
H82	6.9 ± 0.18	27 ± 7.9	T125T[b]	10	0.56	**420**	12
H209	5.6 ± 0.34	13 ± 4.8	Splice[b]	17	0.05	0.31	**153**
H526	7.4 ± 0.42	57 ± 9.7	Splice[b]	22	**396**	0.87	3.8
H146	>5000	163 ± 5.9	PKKKPLD318fs	39	0.39	**66**	0.60
H1930	1.2 ± 0.21	6.1 ± 2.1	G245R	88	0.67	**39**	1.0

[a]Data from the CCLE portal (https://portals.broadinstitute.org/ccle). [b]*TP53* splice site SNP.

Table S2. Neuroblastoma PDX and cell line xenograft clinical and genomic summary. Related to Figures 2, 6 and 7.

PDX	Sex	Phase of therapy	*MYCN*	ALK	TP53	Other
NB-1643	Male	Diagnosis	Amp	R1275Q	WT	*NF1* splice
COG-N-440x	Female	PD-PM	Amp	WT	WT	SLX4 C1426*, *CIC* del
COG-N-421x	Male	PD-PM	Amp	WT	WT	*CDK4* amp
COG-N-453x	Male	PD-PM	Amp	F1174L	WT	
COG-N-471x	Female	PD-PM	Amp	WT	WT	
RH07-1x	n/a	n/a	n/a	n/a	n/a	
Xenograft						
SK-N-AS	Female	PD	Non-amp	WT	del[a]	NRAS Q61K
CHLA-79	Female	PD	Non-amp	WT	WT	ERCC2 E606K

[a]Deletion of one *TP53* allele and expression of C-terminally truncated *TP53* variants from other *TP53* allele due to a deletion in the intron 9/exon 10 junction, although SKNAS cells may maintain some partial TP53 functionality.
PD, Progressive disease; PD-PM, progressive disease-postmortem; Amp, amplified; Non-amp, non-amplified; WT, wild-type; del, deletion; n/a, not available. Comprehensive genomic profiling data for PDXs/xenografts can be found on the PedcBioPortal for Integrated Childhood Cancer Genomics (https://pedcbioportal.kidsfirstdrc.org).

Table S3. Limiting dilution assay growth frequency of SH-SY5Y-Empty and SH-SY5Y-GPC2 isogenic cell dilutions. Related to Figure 2.

Dilution (cells/well)[a]	SH-SY5Y-Empty wells tested	SH-SY5Y-Empty wells with cell growth	SH-SY5Y-GPC2 wells tested	SH-SY5Y-GPC2 wells with cell growth
1000	192	185	192	192
100	192	98	192	150
10	384	192	384	202
1	768	292	768	302

[a]Table represents combined data from 2 independent experiments.

Table S4. Estimation of stem cell frequency in SH-SY5Y-Empty and SH-SY5Y-GPC2 isogenic cells. Related to Figure 2.

1/stem cell frequency[a]	Lower	Estimate	Upper
SH-SY5Y-Empty	45.5	39.8	34.8
SH-SY5Y-GPC2	17.4	15.4	13.6

[a]Calculated with an extreme limiting dilution analysis.[4]

Table S5. D3-GPC2-Fab/ΔHS GPC2$^{24-493}$ X-ray data collection and refinement statistics. Related to Figure 3.

Data collection statistics	
Wavelength (Å)	1.033190
Resolution range (Å)[a]	28.57 - 3.30 (3.42 - 3.30)
Space group	$P2_1$
Unit cell a, b, c (Å) α, β, γ (°)	 54.94 225.65 107.25 90 104.754 90
Total reflections	217,876 (22,809)
Unique reflections	37,835 (3,807)
Multiplicity	5.8 (6.0)
Completeness (%)	99.8 (99.8)
Mean I/sigma(I)	7.3 (1.8)
Wilson B-factor	79.2
R_{merge} (%)[b]	19.1 (76.2)
R_{pim} (%)[c]	8.7 (33.9)
$CC_{1/2}$ (%)	99.1 (82.6)
Refinement Statistics	
Reflections used in refinement	37,816 (3,798)
Reflections used for R_{free}	1,831 (179)
R_{work}[d]/ R_{free}[e]	27.7/ 31.7
Number of non-hydrogen atoms	14,603
Macromolecules	14,603
Protein residues	1,916
RMS_{bonds} (Å)	0.003
RMS_{angles} (°)	0.62
Ramachandran favored (%)	91.9
Ramachandran allowed (%)	7.7
Ramachandran outliers (%)	0.4
Average B-factor (Å^2)	73.9

[a]Statistics for the highest-resolution shell are shown in parentheses

[b]$R_{merge} = \Sigma_{hkl} \Sigma_i | I_{hkl,\ i} - \langle I_{hkl} \rangle | / \Sigma_{hkl} \langle I_{hkl} \rangle$

[c]$R_{pim} = \Sigma_{hkl} [1/(N-1)]_{1/2} \Sigma_i | I_{hkl,\ i} - \langle I_{hkl} \rangle | / \Sigma_{hkl} \langle I_{hkl} \rangle$

[d]$R_{work} = (\Sigma | |F_o| - |F_c| |) / (\Sigma | |F_o| |)$

[e]5% of the data were used for R_{free} calculation

Table S6. D3-GPC2-Fab/ΔHS GPC2$^{24-493}$ interactions. Related to Figure 3.

ΔHS GPC2$^{24-493}$ amino acid residue (BSA)[a]	GPC2 AA	Murine Gpc2 AA	GPC1 AA	GPC3 AA	GPC4 AA	GPC5 AA	GPC6 AA	GPC2 mutant	GPC2 mutant K_D (nM) (fold-change K_D from WT ΔHS GPC2$^{24-493}$)	Interaction type	D3-GPC2-Fab amino acid residue[a]
Asp91 (**14**)	D	D	D	R	E	T	E				
Asp91^{O}										HB	H-Tyr32^{OH}
Thr/Ser92 (**10**)	S	S	S	L	Q	S	T				
Thr/Ser92^{O}										HB	H-Tyr32^{OH}
Phe95 (**76**)	F	F	V	G	H	T	F	F95V	7.1 (7.6)		
Phe95										VDW	H-Asp31, H-Tyr32, H-Ser96, H-Gly97
His98 (**85**)	H	H	A	W	A	F	T				
His98^{ND1}										HB	H-Ser96^{O}
His98										VDW	H-Ser96, H-Gly97, H-Tyr98, L-Tyr49
Thr99 (**6**)	T	T	M	V	V	L	T				
Thr99^{OG1}										HB	H-Gly97^{O}
Thr99										VDW	H-Gly97, H-Tyr98
Ala102 (**45**)	A	A	T	-	S	R	S				
Ala102										VDW	H-Tyr98, H-Asp99, L-Trp32
Arg103 (**6**)	R	R	Q	-	R	N	R	R103Q	2.8 (3.0)		
Arg103$^{NH1, NH2}$										SB	H-Asp99$^{OD1, OD2}$
Arg103										VDW	H-Asp99
Arg105 (**50**)	R	R	R	T	K	A	K				
Arg105										VDW	H-Tyr98, L-Trp32
Lys106 (**85**)	K	K	S	P	K	A	K	K106S	6.7 (7.2)		
Lys106^{NZ}										SB	H-Asp99^{OD2}
Lys106^{NZ}										HB	L-Leu91^{O}
Lys106										VDW	H-Asp103, L-Trp32, L-Asn92
Glu109 (**51**)	E	E	D	E	E	E	E				
Glu109$^{OE1, OE2}$										HB	L-Trp32^{NE1}
Glu109										VDW	L-Ser30, L-Trp32
Thr380 (**35**)	T	T	P	H	T	T	T				
Thr380										VDW	L-Ser28

Thr381 (**40**)	T	T		-	V	T	R	T				
Thr381^{OG1}											HB	L-Ser28^{O}
Thr381											VDW	L-Ser28
Ala382 (**61**)	A	A		-	E	A	N	A				
Ala382											VDW	L-Gln27, L-Ser28, L-Asn92
Arg389 (**16**)	R	R		K	S	R	N	R				
Arg389											VDW	H-Tyr58 L-Tyr94
Trp392 (**26**)	W	W		S	R	T	K	T				
Trp392											VDW	H-Thr56
Glu396 (**101**)	E	E		A	Q	D	N	E	E396A	5.5 (5.9)		
Glu396$^{OE1, OE2}$											HB	H-Tyr33^{OH}, H-Ser52^{OG}, H-Ser55^{N}
Glu396											VDW	H-Tyr33, H-Ser52, H-Ser52A, H-Ser53, H-Ser55
Arg397 (**104**)	R	R		Q	K	K	S	K	R397Q	1573 (1688)		
Arg397$^{NH1, NH2}$											SB	H-Glu95$^{OE1, OE2}$, H-Asp99^{OD1}
Arg397^{NH1}											HB	H-Gly97^{O}
Arg397											VDW	H-Tyr33, H-Glu95, H-Gly97, H-Asp99
Arg400 (**88**)	R	R		D	S	Q	L	L	R400D	26 (28)		
Arg400$^{NH2, NE}$											SB	H-Asp31$^{OD1, OD2}$
Arg400											VDW	H-Ser30, H-Asp31, H-Ser52A
Thr411 (**40**)	T	T		T	Y	N	Q	T				
Thr411											VDW	H-Thr28
Asp415 (**53**)	D	D		E	H	D	N	D				
Asp415											VDW	H-Gly26

[a]Superscript NH1, NH2, NE, OE1, OE2, OG1, OD1, OD2 and O represent the respective atom of amino acid residue involved in interaction. BSA, buried surface area; HB, hydrogen bond; SB, salt bridge; VDW, Van der Waals contact; WT, wild-type; AA, amino acid. The Clustal Omega tool[5] (https://www.ebi.ac.uk/Tools/services/web_clustalo/toolform.ebi) was used to align murine Gpc2 and human GPC1-6 protein sequences. Blue boxes indicate GPC2 identical amino acids for murine Gpc2 and human GPC1 and GPC3-6.

Supplemental References

1. Rajasekaran, S., Nagarajha Selvan, L.D., Dotts, K., Kumar, R., Rishi, P., Khetan, V., Bisht, M., Sivaraman, K., Krishnakumar, S., Sahoo, D., et al. (2019). Non-coding and Coding Transcriptional Profiles Are Significantly Altered in Pediatric Retinoblastoma Tumors. Front Oncol 9, 221.
2. Chai, P., Jia, R., Jia, R., Pan, H., Wang, S., Ni, H., Wang, H., Zhou, C., Shi, Y., Ge, S., et al. (2018). Dynamic chromosomal tuning of a novel GAU1 lncing driver at chr12p13.32 accelerates tumorigenesis. Nucleic Acids Res 46, 6041-6056.
3. Aldiri, I., Xu, B., Wang, L., Chen, X., Hiler, D., Griffiths, L., Valentine, M., Shirinifard, A., Thiagarajan, S., Sablauer, A., et al. (2017). The Dynamic Epigenetic Landscape of the Retina During Development, Reprogramming, and Tumorigenesis. Neuron 94, 550-568 e510.
4. Hu, Y., and Smyth, G.K. (2009). ELDA: extreme limiting dilution analysis for comparing depleted and enriched populations in stem cell and other assays. J Immunol Methods 347, 70-78.
5. Sievers, F., and Higgins, D.G. (2018). Clustal Omega for making accurate alignments of many protein sequences. Protein Sci 27, 135-145.